Development of a Liquefied-gas Micro-satellite Propulsion System Part II – Experimental Evaluation

R.B. Weyer, R.T. Dobson and K. van der Westhuizen

The experimental laboratory work done in the development of a liquefied-gas micro-satellite propulsion system is presented. An experimental model of a thruster system was designed, built and tested using butane as the propellant. Peak thrusts of approximately 50 mN were measured for testing in atmospheric conditions with a starting pressure of between 270 and 290 kPa. By testing in a vacuum chamber environmental back pressures of down to 20 kPa were obtained. An equation to correlate the experimental data was developed. This correlated most of the experimental data to within ± 25 %.

NOMENCLATURE

a	constant
b	constant
c	constant
c_p	specific heat at constant pressure, kJ/kg·K
F_T	thrust, N
$\overline{F_T}$	average thrust, N
g	gravitational acceleration, m/s^2
h_{fg}	enthalpy, kJ/kg·K
I_{sp}	specific impulse, s
m	mass, kg
p	pressure, Pa
R^2	coefficient of determination from multi-linear regression analysis
t	time, s
x	independent variable
y	dependant variable

Greek symbols

γ	specific heat ratio (c_p/c_v)

Subscripts

fg	difference in property between saturated liquid and saturated vapour
liq	liquid
sat	saturated
vap	vapour

1. Introduction

In Part I of this article a theoretical model whereby the performance (specific thrust) of a liquefied-gas propulsion system suitable for attitude control of a micro-satellite may be theoretically predicted was presented. In this paper, Part II, the design, manufacturing and testing of an experimental model is presented. The basic objective of this experimental model is to allow detailed aspects of the two-phase flow and heat transfer to be studied as well as to serve as an experimental benchmark whereby the theoretical model may be verified. Most of the model was constructed from perspex to make it possible to observe the propellant behaviour inside the tank and tubing. In particular it was desired to observe the boiling and two-phase flow behaviour of the working fluid.

Researchers at the University of Surrey have performed work on butane thruster systems. Gibbon and Underwood (2001) discuss the development of a butane system that was successfully used on board the nano-satellite SNAP-1. Using 32.6 grams of butane the thruster system was able to raise the spacecraft's orbit by over 3 km, which related to an effective *delta-V* of between 1.9 and 2.1 m/s. The mission specific impulse and effective thrust were calculated to be 43 s and 46 mN respectively.

Gibbon and Underwood (2001) also put forward recommendations for building a butane propulsion system that could be used onboard a micro-satellite. These include using a conventional tank in which to store the butane (as opposed to the coiled tube arrangement used on SNAP-1) and to perform heating of the fuel in a separate thrust chamber assembly rather than just heating the nozzle.

2. Experimental Model

The experimental model was designed, manufactured and tested in order to verify thruster performance. This would make it possible to compare theoretical predictions with experimental results. The experimental model incorporated locally available components that were relatively cheap (when compared to space-qualified components). The focus of the experimental testing was to prove the concept and verify theoretical results, rather than to qualify the design of the thruster system. Tests were carried out under both ambient and near-vacuum conditions in a vacuum chamber. Most of the model was constructed from perspex to make it possible to observe the propellant behaviour inside the tank and tubing. In addition, the low Young's modulus of Perspex (E=3x10^9 N/m^2) was also appropriate for the method used to measure thrust as discussed in section 3.1. From a manufacturing point of view perspex is a difficult material to work with as it is brittle and has low strength (yield strength typically 50 MPa). Frequent breaking of components occurred during machining and handling. In addition special teflon ferrules had to be manufactured for use on the Perspex tubing when connecting it to brass pipe connector fittings. This was because the standard brass ferrules supplied with the fittings could not be used as they would have cracked the perspex. It was also noted there was an adverse reaction of the perspex to the butane. After a few weeks of testing many fine cracks and stress lines could be seen on parts on the perspex, particularly in the storage tank. However, the damage was only on the surface and did not directly result in any material failures occurring.

The assembled model was mounted to a perspex base plate that was bolted horizontally onto the mounting block inside the

Department of Mechanical Engineering, University of Stellenbosch, South Africa, Email rtd@sun.ac.za

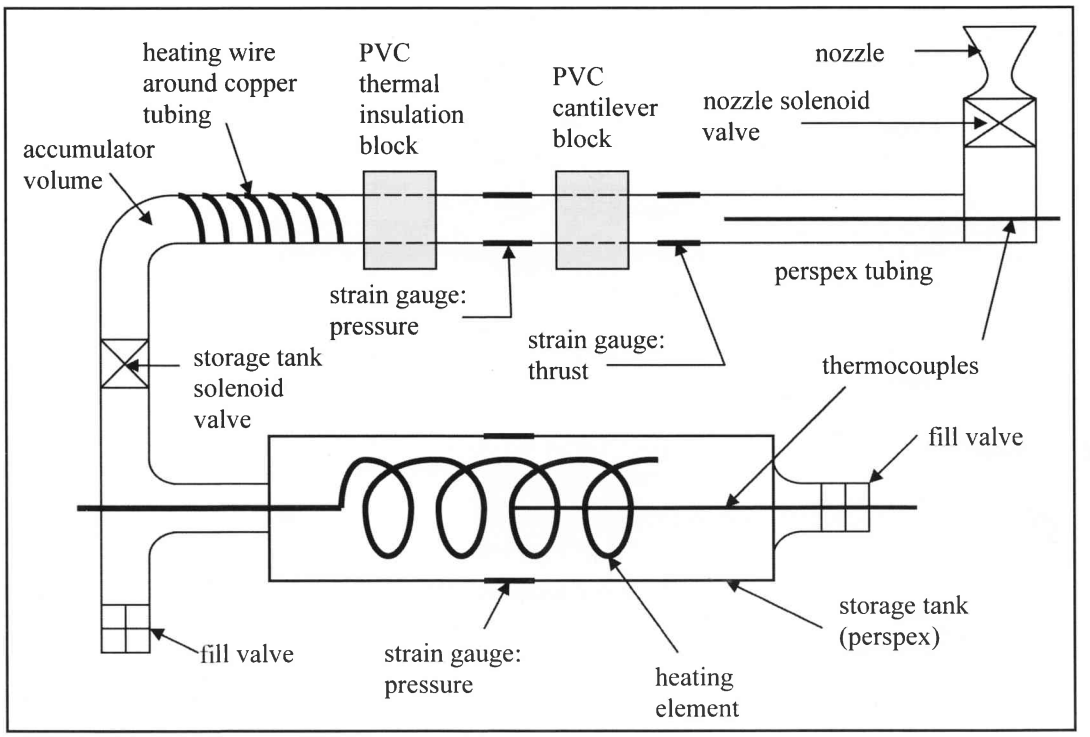

Figure 1: Schematic diagram of experimental model

vacuum chamber.

A schematic diagram of the experimental model is shown in Figure 1, an isometric assembly drawing can be seen in Figure 2 and a photographic image is given in Figure 3. The vacuum chamber and vacuum pump are shown in Figure 4.

3. Test procedure

The storage tank was filled with liquid butane. The storage tank solenoid valve was opened and liquid fed to the heating chamber (accumulator) – usually until the pressures in the heating chamber and storage tank equalised. The saturation temperatures of butane are relatively low (compared to water) - at 200 kPa the saturation temperature is 20°C and at 300 kPa it is 32°C. The typical room temperature at which testing was conducted was 20°C. Thus, for the butane at a pressure lower than approximately 200 kPa, boiling would commence due to heat transfer from the surrounding air to the butane. The model was fitted with two sources of electrical heating energy. A heating element was placed inside the storage tank. This heating element was constructed by placing a length of resistance heating wire inside a copper tube. A hole was drilled into a T-piece connected to the storage tank. The heating element was pushed through this hole and soldered to the T-piece. The other heating element was made by winding insulated resistance heating wires around the copper tubing through which the propellant was fed. The resistance heating wires were electrically insulated from the copper using ceramic beads. In addition the resistance heating wire on the outside of the copper tube was thermally insulated from the environment using asbestos insulation tape. Both heating elements were connected to a variable power supply. Hence, the heat input to the system could be controlled. The boiling propellant resulted in an increase in temperature and pressure that were monitored. Superheating of the vapour also occurred depending on the amount of heat input and the vapour pressure. Once a satisfactory state of pressure had been reached the second solenoid valve was opened, allowing the propellant to flow out the nozzle creating

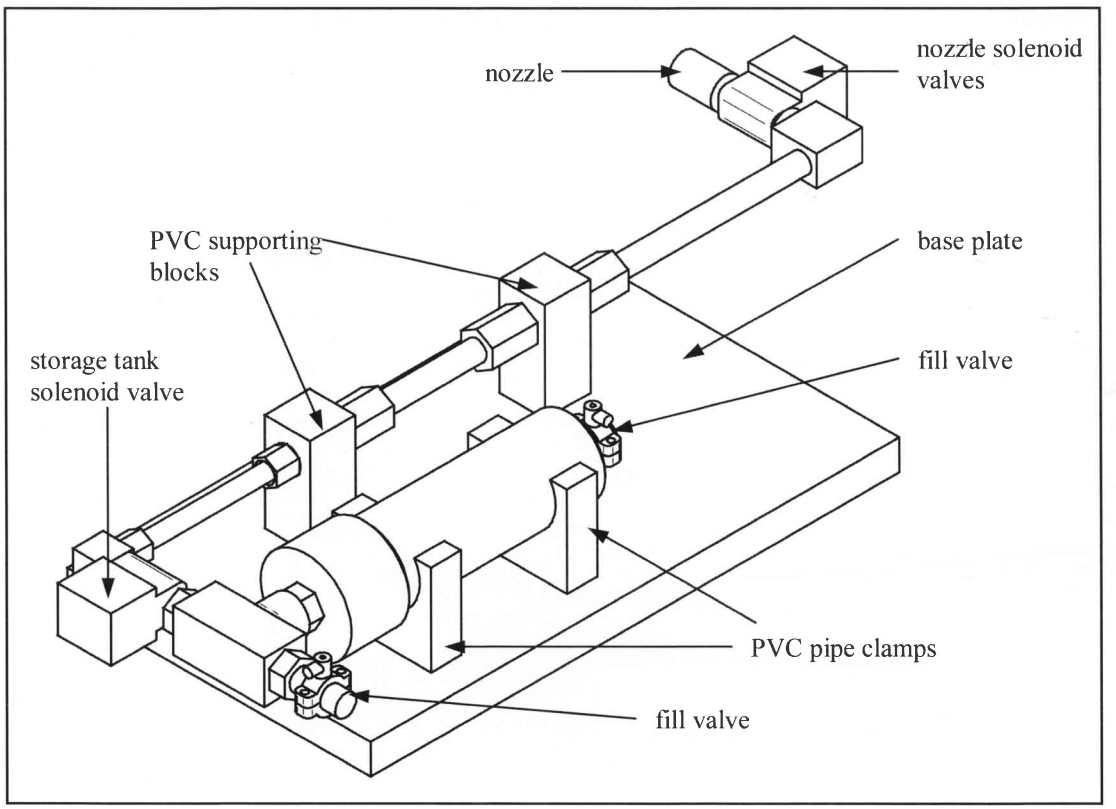

Figure 2: Isometric assembly drawing of experimental model

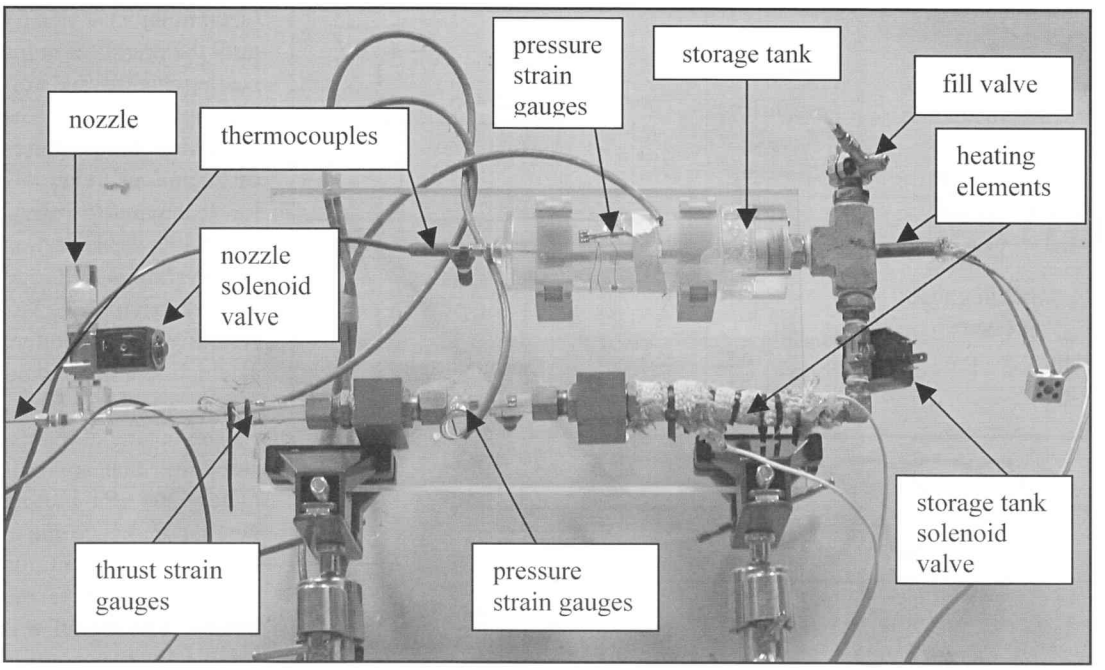

Figure 3: Photograph of experimental model

a thrust on the tube in the opposite direction to that of the flow.

3.1 Thrust Measurement

Accurate determination of the thrust delivered is an important aspect of the experimental work. Due to the fact that the thrust produced is relatively small (in the order of 0.01 N), special consideration had to be given to the method used to measure the thrust. Conventional methods to measure thrusts of much larger magnitudes are not appropriate because the resolution of such measurements is too coarse for the accuracy required. The method that was employed is similar to that used by Ye et al. (2001) in that a cantilevered beam was used. However, whereas Ye et al. (2001) had the thruster firing onto the tip of the cantilevered beam, for the laboratory work conducted for this project the thruster was physically mounted to the end of the cantilevered beam. In addition the cantilever beam was the propellant tubing itself, similar to the method used by Mukerjee et al. (2000). An illustration of this measurement technique is shown in Figure 5. The tube carrying the propellant is cantilevered on one end. The other end is fitted with an elbow fitting causing a 90° change in direction of the propellant. Thus, the thrust force is at right angles to the cantilevered tube. This produces a tip load on the cantilevered tube resulting in a bending moment at the support of the cantilevered tube. Hence, the set-up is modelled as a cantilevered beam subjected to a tip load. By mounting a strain gauge on the cantilevered end the strain can be measured. The magnitude of the tip load that would have produced the strains measured can be determined using either traditional solid mechanics (Benham et al., 1999) or by calibration.

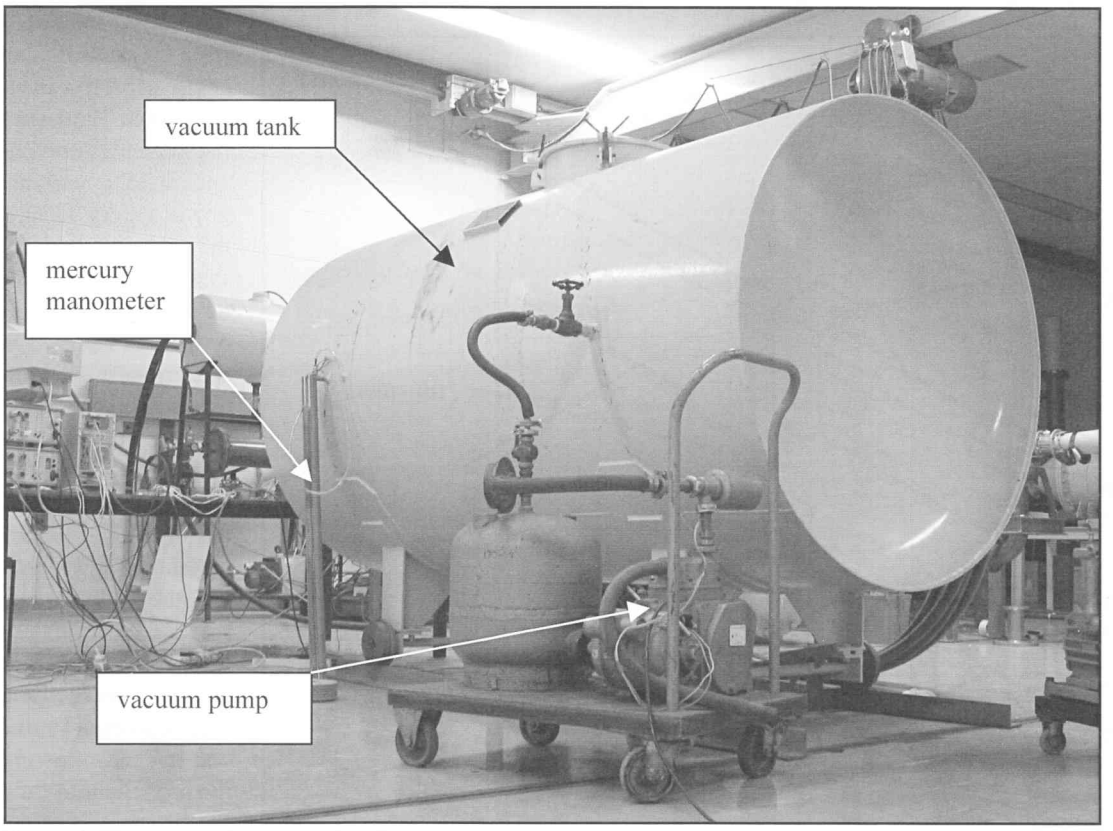

Figure 4: Photograph of vacuum chamber

3.2 Temperature and pressure measurement

Copper-constantan (type T) thermocouples were used to measure the temperatures. Although the use of thermocouples is fairly standard, special attention had to be given to the vacuum chamber connections. Feed-throughs were manufactured which accommodated both copper and constantan wires, to avoid creating a new thermocouple at the junction point. The voltage difference was measured as a differential voltage on one

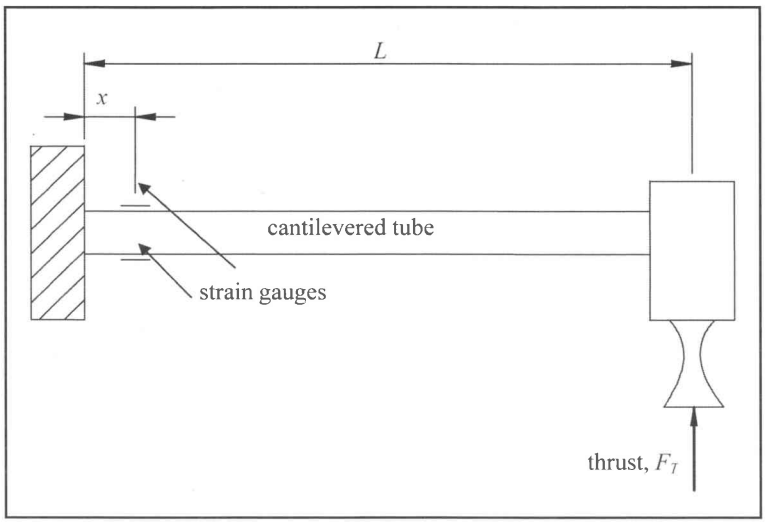

Figure 5: Illustration of method used to measure thrust using cantilevered tube

of the channels of the I/O (*National Instruments PCI-6014 basic multifunction data acquisition board*) card using the configuration software that was supplied with the card to automatically convert the voltage differences to temperature units °C. An ice-bucket was used as to create a reference point at 0°C for one of the junctions since the software required that one junction be at a known temperature. No amplification was done on the thermocouple voltage signal, and hence voltage differences were very small, e.g. 40 μV for a 1°C change in temperature. Unfortunately this was in the same order as the noise on the data acquisition card. In order to eliminate as much of the noise as possible, digital filtering of sampled temperature data was done using a second order Butterworth low-pass filter with a cut-off frequency of 10 Hz.

Pressure measurements were made using strain gauges on both the storage cylinder and accumulator. Although pressure transducers could also have been used, their use would have required that additional connection ports be drilled and fitted onto the storage tank and accumulator. This would (may) have created potential leakage problems. Additionally, pressure gauges are much more expensive that strain gauges. Strain gauges provided a simpler and cheaper option with minimal loss of accuracy. By knowing the strain in a cylindrical pressure vessel, the internal pressure was determined by experimental calibration of the strain gauge bridges using known pressures measured with a pressure transducer (*Hottinger Baldwin Messtechnik*, Type P3MA, Serial No. B14622).

4. Observations and results

Experimental data for butane exhausting to a 100 kPa back pressure is depicted in Figure 6 and Figure 7. The physical parameters of the experimental model are given as the base case values listed in Table 1. The data for Figure 6 was obtained by removing the nozzle valve and operating the storage tank valve, whereas the data in Figure 7 was obtained by keeping the storage tank valve open and operating the nozzle valve. As can be seen in Figure 1 the nozzle valve refers to the solenoid valve between the accumulator and nozzle.

Parameter	Value	Units
Nozzle throat diameter	1	mm
Nozzle exit diameter	5	mm
Storage valve orifice diameter	2.8	mm
Nozzle valve orifice diameter	1.6	mm
Storage tank volume	251.3×10^{-6}	m^3
Accumulator volume	31.5×10^{-6}	m^3
Valve chamber volume	2.36×10^{-6}	m^3

Table 1: Physical parameters of experimental model

It can be seen from Figure 6(a) and Figure 7(a) that whilst similar levels of thrust are obtained, the shape of the thrust curves is different. The solenoid valves operated to generate the thrusts (i.e. the storage tank valve for Figure 6, and the nozzle valve for Figure 7) were both opened at time 1 s and closed at time 3 s. The thrust curves in Figure 7(a) are much steeper at these times (especially when the valves were closed). In Figure 7(a) there was thrust for about 0.5 s after the valve was closed. This is due to the fact that there was some liquid in the accumulator control volume and even after the valve was closed the liquid continued to evaporate providing a supply of gas at a higher pressure than the back pressure.

It is also interesting to examine the pressure graphs (Figure 6(b) (storage tank pressure) and Figure 7(b)). The most important aspect to note is that the pressure recovers after it has dropped due to a firing of the thruster. This is due to the fact that when the butane pressure drops,

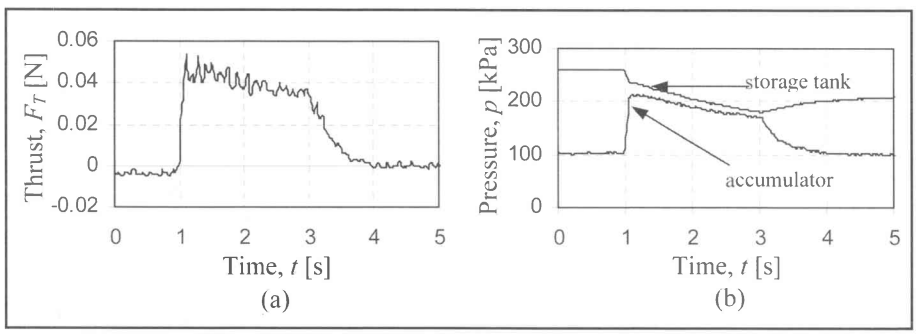

Figure 6: Thrust (a) and pressure (b) against time using storage tank valve

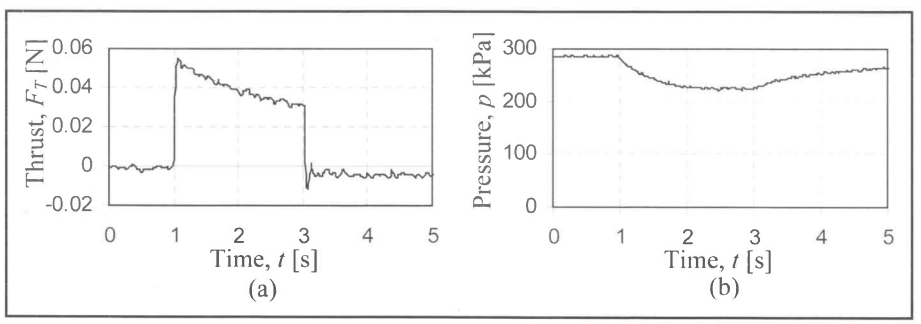

Figure 7: Thrust (a) and pressure (b) against time using nozzle valve

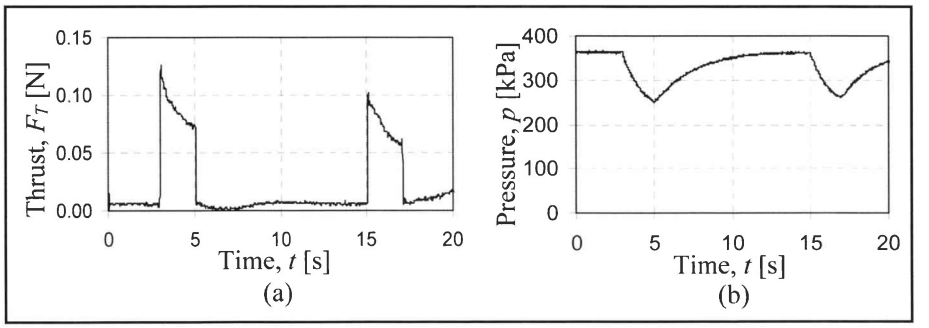

Figure 8: Thrust (a) and pressure (b) vacuum chamber testing (20 kPa) using nozzle valve

the temperature of the liquid butane remaining is higher than the saturation temperature at the new pressure. Hence, liquid butane boils off, causing the pressure to increase until it reaches the saturation pressure corresponding to the temperature of the system. This is what Zakirov et al. (2001) refer to as the *self-pressurising effect* of liquefied-gas systems.

Figure 8 presents the thrust and pressure curves for two consecutive butane firings in a vacuum environment (back pressure of 20 kPa absolute). Although the initial pressure in the system for these firings is about 20 % higher than that in Figure 7(b), the difference between the peak thrust for the vacuum testing is almost double for the test conducted in a 20 kPa environment. It can be seen from Figure 8(b) that the pressure appears to recover almost all of its original value during the ten second interval between the two pulses. However, the peak thrust for the second pulse is somewhat lower that that of the first pulse.

The specific impulse of the butane in the system was estimated experimentally by conducting a test generating a 5 s pulsed thrust as shown in Figure 9. The difference in mass of the liquid butane before and after the pulse was estimated, by observing the drop in the level of the liquid, to be 0.43 grams. The equation used for specific impulse is as follows:

$$I_{sp} = \frac{\overline{F}_T}{\frac{\Delta m}{\Delta t} g} = \frac{\left(\int_0^t F dt\right)/\Delta t}{\frac{\Delta m}{\Delta t} g} \qquad (1)$$

Using equation (1) the specific impulse is calculated as

$$I_{sp} = \frac{0.03}{\frac{430 \times 10^{-6}}{5} 9.81} = 36 \text{ s}$$

The specific impulse I_{sp} as calculated using equation (1) gives a relative measure of how well the energy in the butane is being converted into thrust. The experimental value reported by Gibbon and Underwood (2001) was 43 s, about 20 % higher than the value of 36 determined for the curve in Figure 9.

Figure 10 shows comparisons between theoretically predicted and experimentally measured results. It can be seen in Figure 10(a) that the theoretical model tends to slightly over-predict the measured thrusts. It can also be seen that the discrepancy between theoretical and experimental results increases at lower starting pressures. A correlation between theory and experiment is also shown in Figure 10(b), with the largest discrepancy occurring at the lowest back pressure. In general, judging from the results in Figure 10, it can be seen that the theoretical model was in fact reasonably accurate in predicting thrusts.

Correlation for Experimental Data

In order to generate a correlation between initial pressure and duration of thrust, data from a number of experiments was used to generate a function describing the average thrust as a function of starting pressure and duration of thrust. It is important to note that for this purpose the thrust value used was the *average thrust*, defined as

$$\overline{F}_T = \frac{\int F_T dt}{\Delta t} \qquad (2)$$

It was assumed that the expression correlating average thrust in terms of pulse duration and pressure could be given by

$$y = a x_1^b x_2^c \qquad (3)$$

where y is the dependant variable (average thrust) which is a function of two independent variables x_1 and x_2 (pulse duration and initial pressure), and a, b and c are the constants. These constants are determined by performing a multi-linear regression analysis. The coefficient of determination R^2 indicating the accuracy of the fit was also calculated. The values for a, b, c and R^2 are given in Table 2. Examination of this table reveals that the value of b is much smaller than that of c (about 200 times) and is very

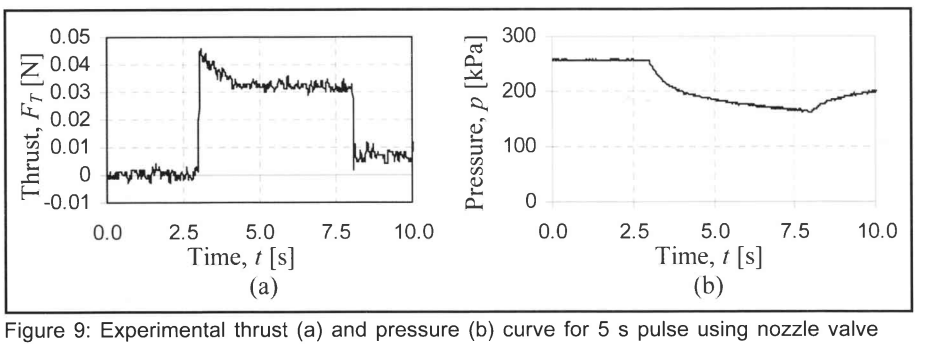

Figure 9: Experimental thrust (a) and pressure (b) curve for 5 s pulse using nozzle valve

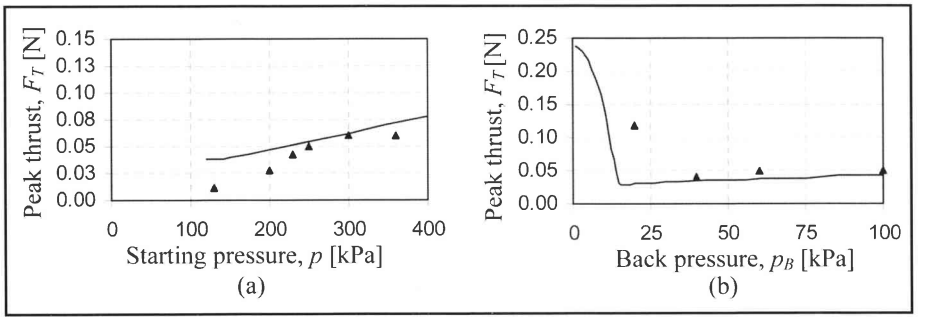

Figure 10: Theoretical and experimental peak thrust as a function of starting pressure (a) and back pressure (b)

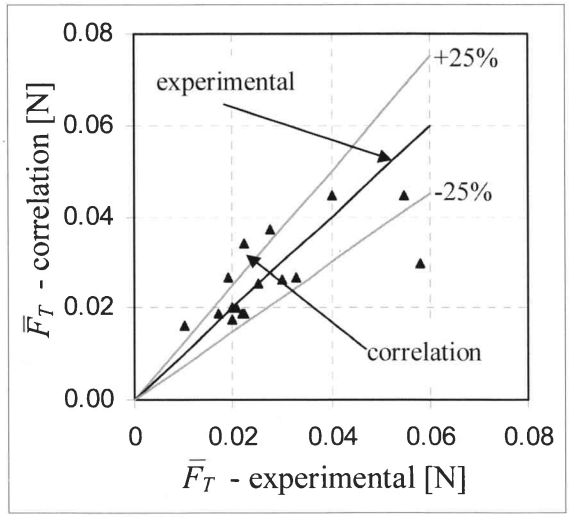

Figure 11: Graphical comparison between experimental data and correlation

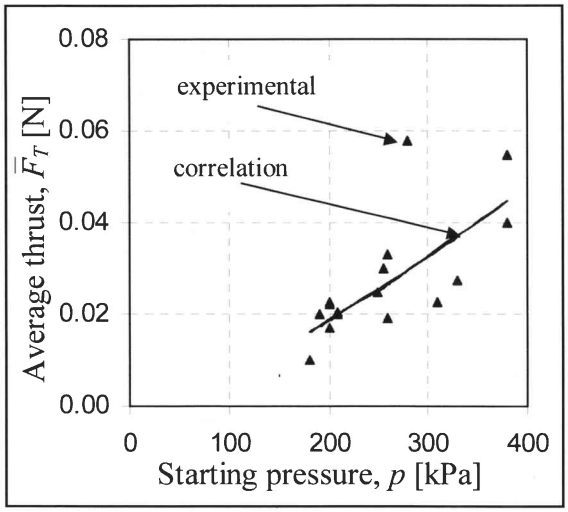

Figure 12: Experimental and correlated average thrust against starting pressure

close to zero. Hence, it is clear that x_2 (initial pressure) is the dominant variable in the correlation. In order to verify this, two further multi-linear regression analyses were performed assuming average thrust to be a function of pulse duration only (c = 0) and of initial pressure alone (b = 0). These results can also be found in Table 2. It can be seen that a low R^2 value of 0.14165 was obtained when average thrust is correlated as a function of pulse duration only – indicating a poor correlation. However, the results for the correlation using initial pressure as the only independent variable are very similar to that obtained using two independent variables. Hence, the following equation can be used to predict average thrust $\bar{F}_T$ in N as a function of the initial pressure p in kPa:

$$\bar{F}_T = 13.706 \times 10^{-6}\, p^{1.36229} \qquad (4)$$

	a	b	c	R^2
$\bar{F}_T = at^b p^c$	12.870×10^{-6}	0.007027	1.37199	0.56364
$\bar{F}_T = at^b p^0$	0.03525	-0.25313	0	0.14165
$\bar{F}_T = at^0 p^c$	13.706×10^{-6}	0	1.36229	0.56356

Table 2: Values for correlation as function of pulse duration and initial pressure

Using the correlation given in equation (4) Figure 11 and Figure 12 are given to present graphically the accuracy with which equation (4) correlates the experimental data from which it was obtained. In Figure 11 it can be seen that the correlation appears to work reasonably well. There is one stray experimental data point for a 0.06 N average thrust. However, this was for the highest experimental average thrust used and is thus at the limit of the range. The comparison between the experimental data and the correlation against initial pressure shown in Figure 12 indicates a fair amount of scattering of the experimental data points about the correlation curve. Whilst a better correlation may have been obtained for Figure 12 had average pressure, rather than starting pressure, been used as the independent variable, the starting pressure is a system parameter than can be controlled and set as opposed to average pressure which is a parameter that a user cannot specify before a firing.

5. Discussions and Conclusions

The experimental work aspects in developing a liquefied-gas micro-satellite propulsion system have been presented. Typical results for butane firings from a pressure of 200 to 300 kPa into a back pressure of 100 kPa showed a peak thrust of about 50 mN, dropping off to about 30 mN over a period of two seconds (see for example Figure 6, Figure 7 and Figure 9). The peak thrust of 50 mN agrees well with the measured value of 46 mN for butane at 200 kPa reported by Gibbon et al (2000). The correlation of numerical and experimental data was reasonable for butane, and theoretical results for steady thrust were typically 30 % higher than that measured experimentally (compare the theoretical results in Figure 8 of Part I to the corresponding experimental result in Figure 7).

The method used to measure thrusts (section 3.1) was relatively simple and low cost in comparison to most of the other methods discussed in section 3.1. The only specialist equipment required was a bridge amplifier and a data acquisition card. In addition no numerical differentiation or integration of the signal was required, as would have been the case had a method using an accelerometer been used (for example in the method used by Ziemer et al. (1997). However, the method used does have a number of limitations. A material with a very low Young's modulus must be used in order to ensure that the structure is flexible enough to be affected by the

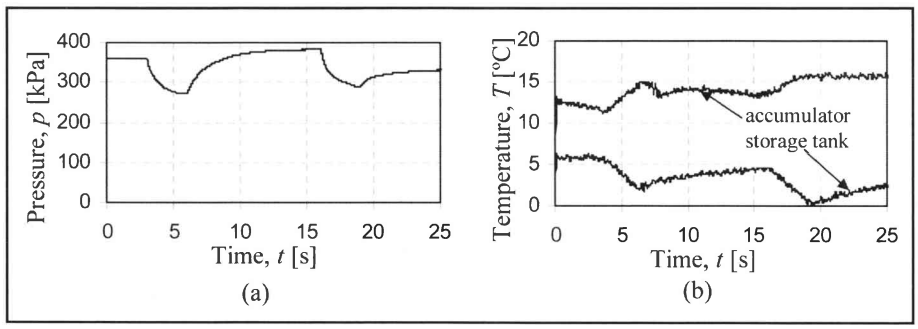

Figure 13: Pressure (a) and temperature (b) for two pulses of three seconds

relatively low thrusts produced. In addition this method is susceptible to factors such as strain gauge alignment, vibration of the solenoid valve and nozzle after opening and closing and additional stiffness added to the system by electrical wiring (strain gauges, thermocouples and valve power supply).

For the experimental work butane used for refilling cigarette lighters was used for reasons of availability, cost and convenience. However, this butane is a mixture of normal butane, iso-butane and propane. The mixture ratio given by the manufacturer is: 54% normal butane, 24 % iso-butane and 22 % propane. A comparison of various saturation properties for normal butane, iso-butane and propane at 10 °C is given in Table 3. It can be seen that at the given temperature the corresponding saturation pressure is approximately 50 % higher for iso-butane than for normal butane, and almost 5 times higher than for propane. This explains why the temperature values shown in Figure 13 are higher than the values given by tabulated data for the saturation properties corresponding to the given pressure for pure normal butane.

	$p_{sat@T}$ [kPa]	h_{fg} [kJ/kg]	c_{p_vap} [kJ/kg·K]	c_{p_liq} [kJ/kg·K]	γ
normal butane	148.7	376.1	1.705	2.367	1.123
iso-butane	220.1	345.8	1.705	2.363	1.136
propane	636.5	359.9	1.869	2.591	1.219

Table 3: Comprison of various properties of saturated normal butane, iso-butane and propane at 10 °C

The experimental work conducted for this project used cheap locally available components. Nevertheless, reasonable experimental results were obtained that compared well to those given by Gibbon and Underwood (2001). This serves to stress the usefulness of even relatively crude practical models in establishing a baseline from which to further develop a thruster system. However, it is recommended that a system incorporating as many of the actual components intended to be flown in space be designed and built for experimental testing as this would be necessary in making the system eligible to be considered for space flight applications.

Acknowledgements

The authors would like to acknowledge the partial financial support given by Sunspace Systems (Pty) Ltd.

References

1. *Benham, P.P., Crawford, R.J., Armstrong, C.G.,* Mechanics of Engineering Materials, *Longman, London, 1999*
2. *Gibbon, D., Underwood, C.,* Low cost butane propulsion systems for small spacecraft, *Proceedings of the 15th Annual AIAA/USU Conference on Small Satellites, Logan, Utah, 2001*
3. *Gibbon, D., Ward, J., Kay, N., The Design,* Development and Testing of a Propulsion System for the SNAP-1 Nanosatellite, *Proceddings of the 14th Annual AIAA/USU Conference on Small Satellites, Logan, Utah, 2000*
4. *Mukerjee, E.V., Wallace, A.P., Yan, K.Y., Howard, D.W., Smith, R.L., Collins, S.D.,* Vaporizing liquid microthruster, *Sensors 83, 2000, pp. 231 – 236*
5. *Ye, X.Y., Tang, F., Ding, H.Q., Zhou, Z.Y.,* Study of a vaporizing water micro-thruster, *Sensors and Actuators A89, 2001, pp. 159 - 165*
6. *Zakirov, V., Sweeting, M., Erichsen, P., Lawrence, T.,* Specifics of Small Satellite Propulsion: Part I, *Proceedings of the 15th Annual AIAA/USU Conference on Small Satellites, Logan, Utah, 2001*
7. *Ziemer, J.K., Cubbin, E.A., Choueiri, E.Y., Birx, D.,* Performance Characterisation of a High Efficiency Gas-Fed Pulsed Plasma Thruster, *AIAA-97-2925, Proceedings of the 33rd AIAA Joint Propulsion Conference, Seattle, Washington, 1997*